Hyperthermia-Mediated Local Drug Delivery by a Bubble-Generating Liposomal System for Tumor-Specific Chemotherapy

Ko-Jie Chen,[†,¶] Er-Yuan Chaung,[†,¶] Shiaw-Pyng Wey,[‡,¶] Kun-Ju Lin,[‡,§] Felice Cheng,[⊥] Chia-Chen Lin,[†] Hao-Li Liu,[∥] Hsiang-Wen Tseng,[⊥] Chih-Peng Liu,[⊥] Ming-Cheng Wei,[⊥] Chun-Min Liu,[⊥] and Hsing-Wen Sung[†,*]

[†]Department of Chemical Engineering and Institute of Biomedical Engineering, National Tsing Hua University, Hsinchu 30013, Taiwan, ROC, [‡]Department of Medical Imaging and Radiological Sciences and Institute for Radiological Research, Chang Gung University, Taoyuan 33302, Taiwain, ROC, [§]Department of Nuclear Medicine and Molecular Imaging Center, Chang Gung Memorial Hospital, Taoyuan 33302, Taiwain, ROC, [⊥]Biomedical Technology and Device Research Laboratories, Industrial Technology Research Institute, Hsinchu 30013, Taiwain, ROC, and [∥]Department of Electrical Engineering, Chang Gung University, Taoyuan 33302, Taiwain, ROC. [¶]These authors contributed equally to this work.

ABSTRACT As is widely suspected, lysolipid dissociation from liposomes contributes to the intravenous instability of ThermoDox (lysolipid liposomes), thereby impeding its antitumor efficacy. This work evaluates the feasibility of a thermoresponsive bubble-generating liposomal system without lysolipids for tumor-specific chemotherapy. The key component in this liposomal formulation is its encapsulated ammonium bicarbonate (ABC), which is used to actively load doxorubicin (DOX) into liposomes and trigger a drug release when heated locally.

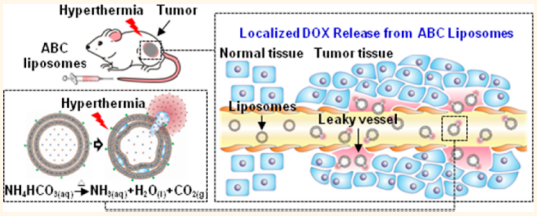

Incubating ABC liposomes with whole blood results in a significantly smaller decrease in the retention of encapsulated DOX than that by lysolipid liposomes, indicating superior plasma stability. Biodistribution analysis results indicate that the ABC formulation circulates longer than its lysolipid counterpart. Following the injection of ABC liposome suspension into mice with tumors heated locally, decomposition of the ABC encapsulated in liposomes facilitates the immediate thermal activation of CO_2 bubble generation, subsequently increasing the intratumoral DOX accumulation. Consequently, the antitumor efficacy of the ABC liposomes is superior to that of their lysolipid counterparts. Results of this study demonstrate that this thermoresponsive bubble-generating liposomal system is a highly promising carrier for tumor-specific chemotherapy, especially for local drug delivery mediated at hyperthermic temperatures.

KEYWORDS: thermoresponsive liposome · triggered release · local drug delivery · doxorubicin · biodistribution

Widely recognized for their ability to increase intratumoral accumulation, PEGylated liposomes are employed as stable vehicles for carrying doxorubicin (DOX; Doxil).[1−4] However, the slow and passive drug release from the Doxil formulation (<10% in 24 h) significantly inhibits its antitumor efficacy.[5,6] Therefore, an approach must be developed to actively trigger a drug release from PEGylated liposomes and enhance their therapeutic outcome. A thermoresponsive liposomal formulation (ThermoDox) has been developed that rapidly releases DOX in regions where local tissue temperatures are elevated. ThermoDox contains three lipid components in a 90:10:4 molar ratio: dipalmitoylphosphatidylcholine (DPPC); monostearoylphosphatidylcholine (MSPC), which is a lysolipid; and poly(ethylene glycol) 2000-distearoylphosphatidylethanolamine (PEG 2000-DSPE).[7−9]

The underlying mechanism of the rapid drug release from the ThermoDox formulation is that the lipids (DPPC and MSPC) undergo a gel-to-liquid phase transition in the region of their phase transition temperature (T_m; approximately 41 °C).[10] When heated to 40−42 °C, temperature-induced membrane instability increases the permeability of liposomes, subsequently releasing their encapsulated drugs. Related studies have demonstrated that the ThermoDox formulation performs superior to the Doxil formulation in releasing encapsulated DOX.[7,11,12]

While proven effective in reducing tumor volume in animal models,[7−9] ThermoDox

* Address correspondence to hwsung@che.nthu.edu.tw.

Received for review February 27, 2014 and accepted April 17, 2014.

Published online April 17, 2014
10.1021/nn501162x

has recently begun phase III clinical trials for hepatocellular carcinoma treatment.[7,12] Despite the significant therapeutic potential of ThermoDox, approximately 50% of its encapsulated DOX is released within 1 h in physiological environments.[13,14] As is widely suspected, lysolipid dissociation from the liposomes mediated by plasma proteins contributes to their intravenous instability.[14]

To resolve the above problem, our group recently developed a thermoresponsive liposomal formulation without lysolipids.[15] This thermoresponsive liposomal formulation consists of DPPC, cholesterol, and PEG 2000-DSPE in a molar ratio of 60:40:5. As the key component of this liposomal formulation, its encapsulated ammonium bicarbonate (ABC; NH_4HCO_3) creates the transmembrane gradient needed for a highly efficient DOX encapsulation. Moreover, at a high temperature of roughly 42 °C, ABC decomposition generates CO_2 bubbles,[16−18] subsequently creating permeable defects in the lipid bilayer and ultimately inducing a rapid DOX release to instantly increase the drug concentration locally. Notably, ABC is a raising agent commonly found in the food industry to generate gas bubbles in baked goods.[19] Physiologically, bicarbonate ions are generated in red blood cells and used to maintain a balanced pH; once completing their task, these ions are released by the lungs as CO_2.[20,21]

This work evaluates the feasibility of using this thermoresponsive bubble-generating liposomal system (ABC liposomes) for tumor-specific chemotherapy under mild hyperthermia. Clinically, local hyperthermia may be produced by ultrasound energy, microwave, radio frequency, or using magnetic hyperthermia.[22] The thermosensitive ABC formulation is administered intravenously *via* the tail vein in mice during hyperthermia treatment at roughly 42 °C, thereby triggering the immediate release of the encapsulated drug within the heated tumor. The released drug diffuses into the tumor along a high drug concentration gradient, specifically attacking tumor cells (Figure 1). The control groups consist of liposomes formulated in aqueous ammonium sulfate (AS liposomes), a preparation that resembles the Doxil formulation,[1,23] together with a formulation that resembles that of ThermoDox (DPPC/MSPC/PEG 2000-DSPE = 90:10:4 containing AS; lysolipid liposomes). Moreover, the *in vitro* drug-release profiles are quantified from test liposomes under mild hyperthermia conditions. Their *in vivo* biodistribution, pharmacokinetics, drug accumulation, and antitumor activity against locally heated tumors are examined, as well.

RESULTS AND DISCUSSION

Characteristics of Test Liposomes. The lysolipid, AS, and ABC liposomes were prepared at room temperature by using the lipid-film hydration method, followed by sequential extrusion. Based on their transmembrane AS (or ABC) gradient, a remote-loading technique was applied to load actively DOX into the test liposomes.[23,24] Table 1 summarizes the important formulation characteristics of the as-prepared lysolipid, AS, and ABC liposomes. The three test liposomes had comparable particle sizes, polydispersity indices, and zeta-potentials ($P > 0.05$). An efficient and stable loading of DOX into the aqueous phase of each liposomal formulation (>90%) was attained; additionally, the encapsulated DOX content (approximately 5.0% wDOX/wlipids) was around 100-fold higher than its saturated concentration.[25]

According to the differential scanning calorimeter (DSC) data, the phospholipid composition used to prepare each liposomal formulation significantly influences its phase transition temperature (T_m). While having the same phospholipid components, the AS and ABC liposomes had a significantly higher T_m (52.0 °C) than that of the lysolipid liposomes (41.3 °C; $P < 0.05$). Notably, the T_m value of DPPC-based liposomes is substantially increased when cholesterol is incorporated into their lipid bilayers.[7]

***In Vitro* Drug-Release Profiles.** Figure 2 shows the *in vitro* DOX release profiles from the test liposomes at 37 °C (body temperature) and 42 °C (hyperthermic temperature), which were determined by measuring the increases of their fluorescence intensities in phosphate buffered saline (PBS) over time. As the AS liposomes lacked a triggering mechanism, the amount of DOX released at both temperatures was minimal, indicating that the AS liposomal formulation is relatively stable and its drug release is unaffected by temperature. Incapable of releasing their encapsulated drugs promptly and adequately, the cytotoxic effects of stable liposomal formulations on tumor cells are suboptimal.[5,6]

The amounts of DOX released from the lysolipid and ABC liposomes at 37 °C were relatively low. Nevertheless, when the environmental temperature was heated to 42 °C, significant amounts of their encapsulated DOX were released immediately (within 30 s). This finding suggests that their membrane permeability heavily depends upon the environmental temperature. Including lysolipids (*i.e.*, MSPC) in the lipid bilayer significantly increases the permeability of liposomal membranes at their phase transition temperature.[7−9] Conversely, the ABC liposomes undergo a unique temperature-induced change, triggering their localized drug release. Namely, upon heating to a temperature of ≥40 °C, ABC decomposes quickly and generates CO_2 bubbles, subsequently creating permeable defects in the lipid bilayer and ultimately facilitating the swift release of DOX.[16−18]

Above results demonstrate that the ABC liposomes were relatively stable at 37 °C and could retain their encapsulated drug during blood transport. However,

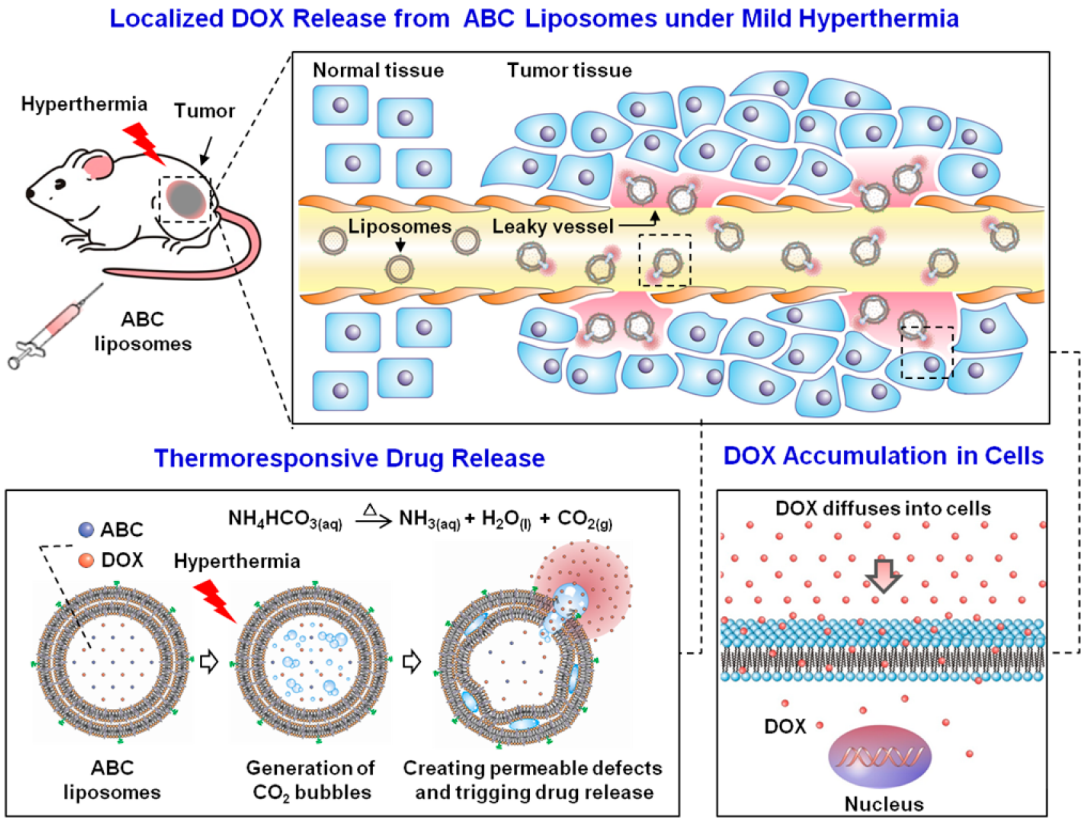

Figure 1. Schematic diagrams showing the composition of the thermoresponsive bubble-generating ABC liposomes with their working mechanism of the action that delivers high concentrations of drug in a tumor region targeted with the application of localized hyperthermia.

TABLE 1. Formulation Characteristics of the Lysolipid, AS, and ABC Liposomes Containing DOX[a]

test samples	diameter (nm)	polydispersity index	zeta-potential (mV)	encapsulation efficiency (%)	encapsulation content (%)	T_m (°C)
lysolipid liposomes	150.9 ± 11.5	0.16 ± 0.04	0.56 ± 0.01	93.4 ± 5.2	4.7 ± 0.3	41.3 ± 0.5
AS liposomes	151.4 ± 9.3	0.17 ± 0.02	−0.11 ± 0.01	94.6 ± 7.3	4.7 ± 0.4	52.0 ± 0.7
ABC liposomes	150.5 ± 12.1	0.15 ± 0.03	−0.12 ± 0.01	96.2 ± 6.1	4.8 ± 0.3	52.0 ± 0.5

[a] The data are presented as mean ± SD ($n = 6$ in each group). Encapsulation efficiency: (mass of DOX in liposomes/mass of DOX in the initial solution) × 100%. Encapsulation content: (mass of DOX in liposomes/mass of lipids) × 100%. T_m: temperature at the transition peak maximum.

when the local temperature was heated to 42 °C, drug release from the liposomes was extremely fast (50% of the encapsulated DOX was released within 30 s; Figure 2), subsequently counteracting the rapid blood passage time and washout from the tumors.[11]

Biodistribution of Test Liposomes. Compared with its counterparts without lysolipids, the lysolipid-containing liposomal formulation has a poor intravenous stability, thus accelerating the plasma clearance.[15] Radionuclide-based molecular imaging modalities such as single-photon emission computed tomography (SPECT) are highly effective for noninvasive visualization, characterization, and quantification of biological processes in living subjects.[26,27] To assess their biodistribution, a direct technetium-99m (^{99m}Tc, a diagnostic radionuclide) labeling method, employing *N*,*N*-bis(2-mercaptoethyl)-*N*′,*N*′-diethylethylenediamine (BMEDA),[28] was applied to identify test liposomes. BMEDA, which is lipophilic at pH 7.4, functions as a lipophilic chelator for ^{99m}Tc to transport the radionuclide across the lipid bilayer of preformed liposomes. Once within the more acidic liposome interior pre-encapsulated with AS or ABC, the pH gradient provides stable entrapment of the ^{99m}Tc-BMEDA complex within the test liposomes (^{99m}Tc-liposomes).[29] Free ^{99m}Tc-BMEDA was then separated from ^{99m}Tc-liposomes using a gel filtration method.[30] Notably, labeling test liposomes with ^{99m}Tc-BMEDA allows us to examine their organ distribution, tumor accumulation, and pharmacokinetics. According to our results, the labeling efficiencies of the lysolipid, AS, and ABC liposomes were 96.9 ± 3.3, 98.0 ± 3.1, and 97.6 ± 3.5% ($n = 6$ in each group), respectively, as analyzed by the instant thin-layer chromatography (ITLC).[31]

Figure 3a shows the biodistribution of the ^{99m}Tc-lysolipid, ^{99m}Tc-AS, and ^{99m}Tc-ABC liposomes in

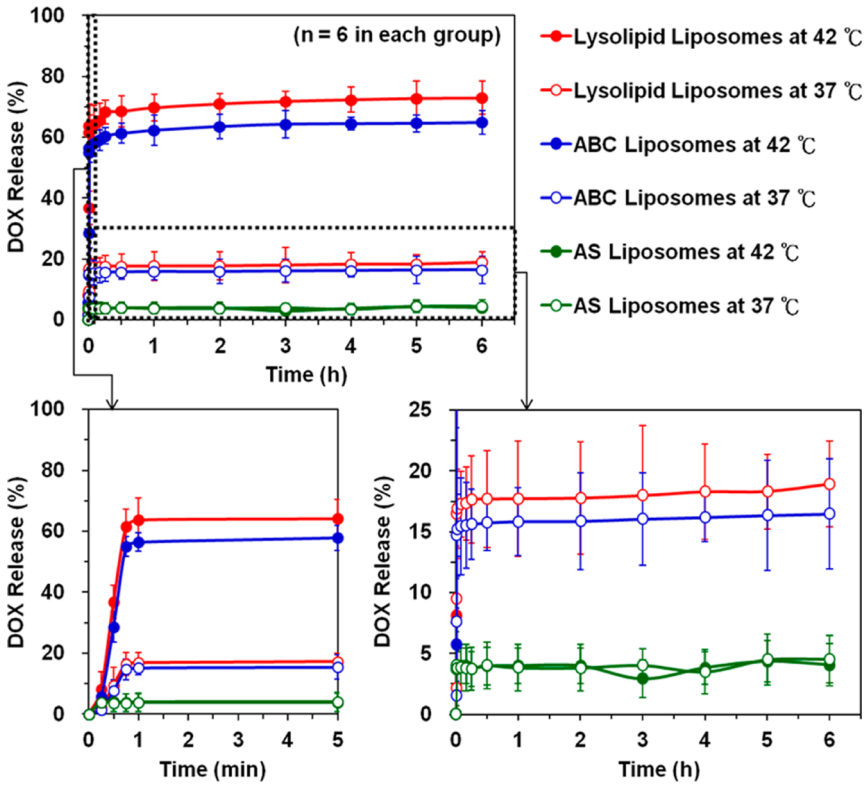

Figure 2. Release profiles of DOX from the lysolipid, AS, and ABC liposomes incubated in PBS at 37 or 42 °C. The lower left-hand side of the figure displays a zoom-in image of drug release in the first couple of minutes, and the lower right-hand side of the figure represents a zoom-in image of drug release in the lower *y*-axis values.

the coronal tomographic views after their intravenous bolus injection in athymic nude mice bearing tumor xenografts at various time intervals. Anatomic locations were identified by superimposing the radioactivity of ^{99m}Tc-liposomes (SPECT images) on the CT images. In the study, tumor xenografts were established in the right flanks of nude mice by injecting them with 5×10^6 H460 human lung cancer cells subcutaneously.[32,33] Previous studies have reported severalpromising results regarding regional hyperthermia in combination with radiotherapy for local treatment of selected lung cancers.[34,35] Figure 3b displays the percentages of injected dose per volume (% ID/mL) accumulated in different organs and tumors.

Immediately after intravenous administration, the radioactivity in test mice that received the ^{99m}Tc-AS or ^{99m}Tc-ABC liposomes was located primarily in the liver. A related investigation has attributed the hepatic uptake of liposomes to phagocytosis by Kupffer cells, which are situated in the liver sinusoids.[36] As time progressed, the level of radioactivity in the liver obviously declined, while high radioactivity in the kidney and bladder was found. According to a related study, liposomes do not permeate to any extent within the kidney.[29] Above results suggest that some of the ^{99m}Tc-BMEDA released from the metabolized liposomes excreted through the kidney and bladder. A related investigation has postulated that liposome metabolism is mediated predominantly by Kupffer cells in the liver.[37]

In contrast, high levels of radioactivity were initially observed in the liver, kidney, and bladder in mice treated with the ^{99m}Tc-lysolipid liposomes. Although their radioactivity in the liver diminished significantly over time, those that accumulated in the kidney and bladder increased relatively. Above findings suggest that the removal of ^{99m}Tc-lysolipid liposomes from blood and the excretion of their metabolized ^{99m}Tc-BMEDA *via* the kidney and bladder were significantly faster than those of ^{99m}Tc-AS and ^{99m}Tc-ABC liposomes. Given their longer circulation half-life, the level of radioactivity accumulated in tumors in mice receiving the AS or ABC liposomes appeared relatively stronger than those treated with the lyoslipid liposomes. Success of the liposome uptake by tumors relies mainly on the enhanced permeability and retention (EPR) effect, which heavily depends on both the size of test liposomes (ranging from 100 to 200 nm in diameter) and their prolonged circulation half-life in the blood.[38]

Plasma Stability. Plasma proteins and cellular membrane pools may be responsible for the destabilization of test liposomes and their drug leakage, thereby affecting their circulation half-life.[16] The stability of different liposomal formulations under physiological conditions was evaluated after incubation with whole

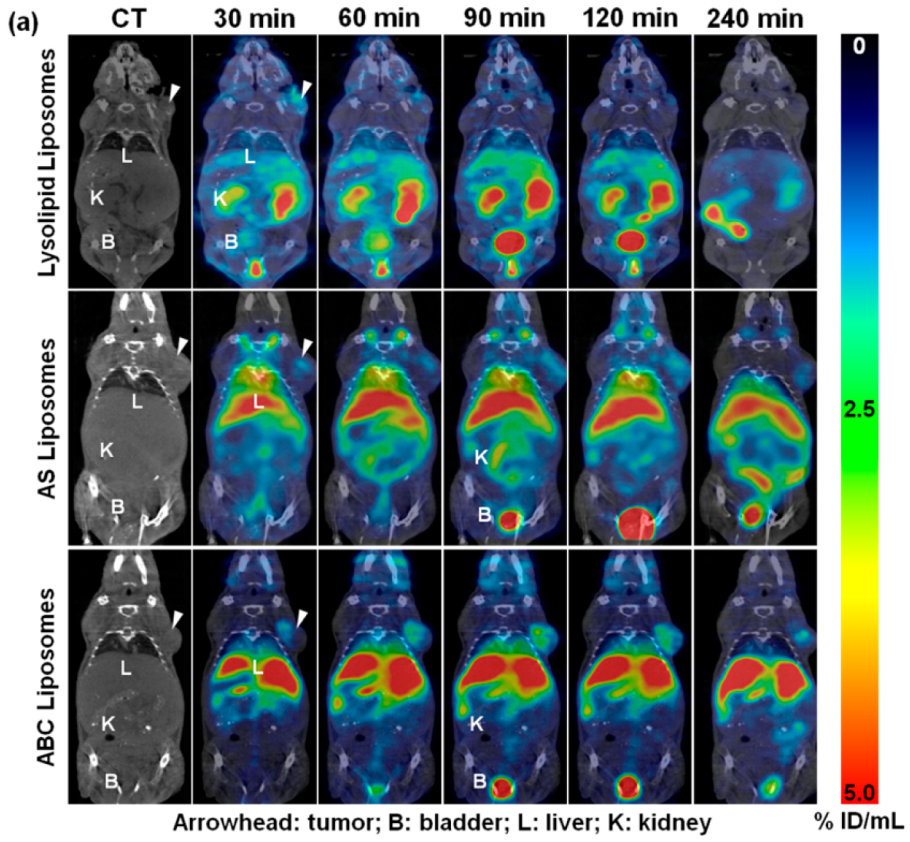

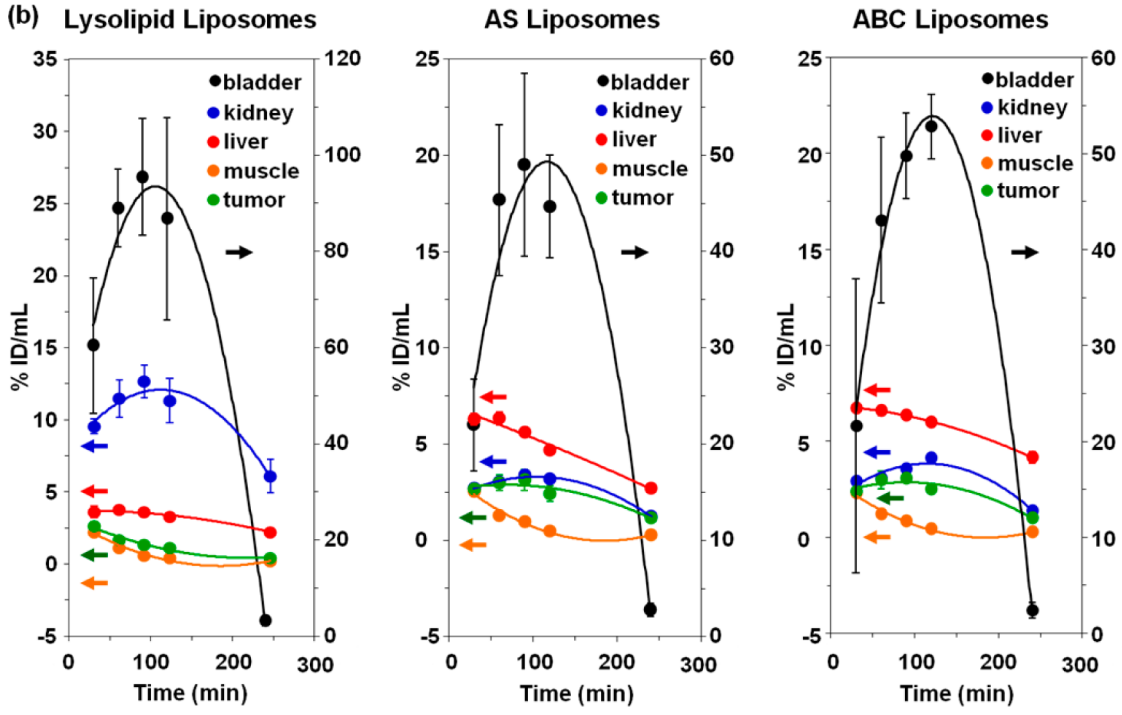

Figure 3. (a) SPECT images showing the biodistribution of the ^{99m}Tc-lysolipid, ^{99m}Tc-AS, and ^{99m}Tc-ABC liposomes in the coronal tomographic views after their intravenous bolus injection in mice at various time intervals; the rainbow pseudocolor scale shows the concentrations of test ^{99m}Tc-liposomes accumulated in different organs and tumors. (b) This figure also shows the percentages of injected dose per volume (% ID/mL) *vs* time profiles of test ^{99m}Tc-liposomes accumulated in the bladder (right *y*-axis), tumor, and other internal organs (left *y*-axis). The decline in radioactivity observed at 240 min was due to the urination of test animals.

blood at 37 °C. In this study, the rat whole blood was used, as the average total blood volume of a mouse is limited (*ca.* 80 mL/kg) and is therefore inadequate for this experiment.[22]

Analytical results (Figure 4) indicate that incubation of the lysolipid liposomes with whole blood significantly decreased the retention of encapsulated DOX ($P < 0.05$); only about 50% of initial DOX remained in the test liposomes after 1 h of incubation. Conversely, without the inclusion of lysolipids, the AS and ABC liposomes retained approximately 90 and 85% of the encapsulated DOX, respectively, at 1 h following incubation with whole blood. Lysolipid dissociation from circulating liposomes is typically mediated by the plasma protein and cellular membrane pools, thus reducing their circulation longevity.[14]

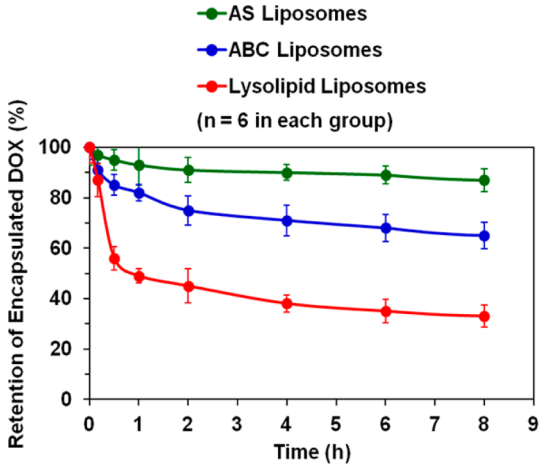

Figure 4. Results of the plasma stability of the lysolipid, AS, and ABC liposomes incubated in whole blood at 37 °C over time.

***In Vivo* DOX Accumulation.** Above experimental results indicate that the AS and ABC liposomal formulations had a greater liposome uptake by tumors than that of the lysolipid liposomal formulation, owing to their prolonged circulation half-life (Figure 3a,b). This study also investigated how local hyperthermia treatment influences the amount of DOX release from the AS and ABC liposomes accumulated in tumors. Test liposomes encapsulated with DOX were first injected intravenously *via* the tail vein in tumor-bearing mice (5 mg liposomes/kg). At 10 min after administration, the tumor site was heated to 42 °C locally using a temperature-controller water mat.[39,40] Hyperthermia (10 min) was interleaved with 5 min cooling periods; this process was repeated for three treatments. At 4 h following treatments, mice were sacrificed, and their organs (including tumor) were harvested. Accumulations of DOX in tissues were visualized by an *in vivo* imaging system (IVIS; Figure 5a), and their fluorescence intensities were quantified using a spectrofluorometer (Figure 5b).

According to Figure 5a,b, the DOX delivered by the AS and ABC liposomes was mainly accumulated in the

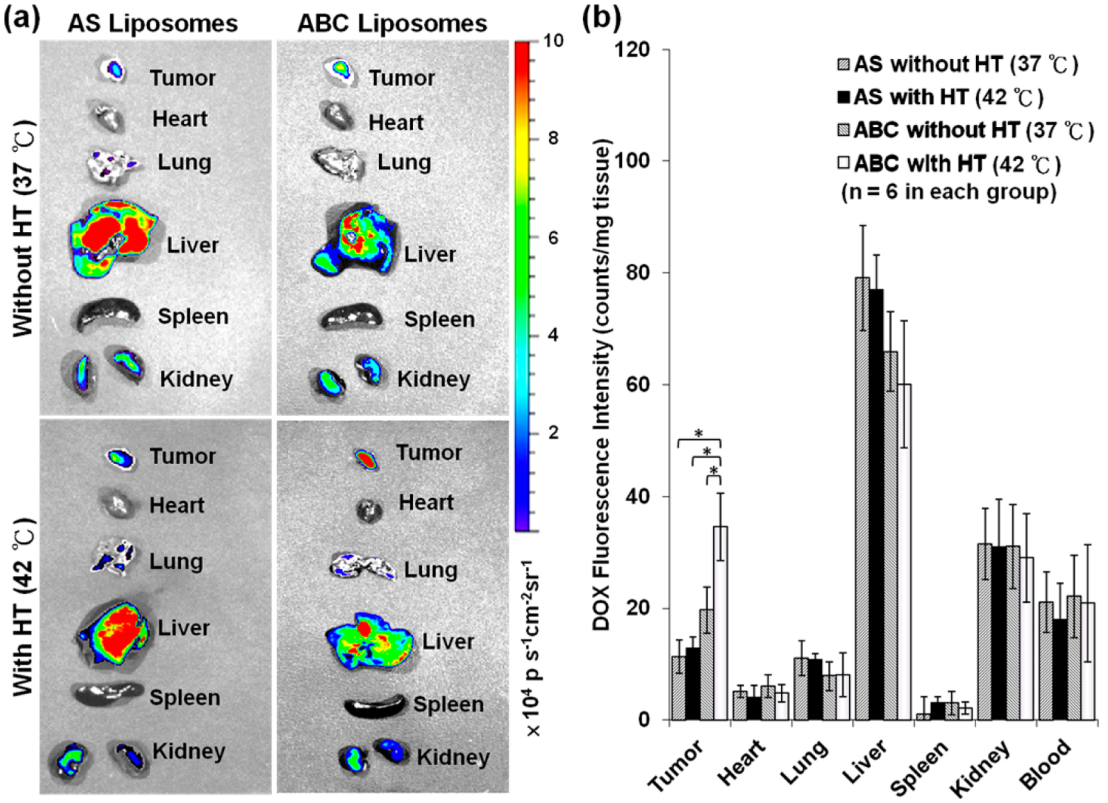

Figure 5. (a) Fluorescent images of DOX of the organs and tumors following intravenous injection of the AS and ABC liposomes with or without hyperthermia treatment in mice and (b) their fluorescence intensities quantified by a spectrofluorometer. *Statistical significance at a level of $P < 0.05$. HT: hyperthermia treatment.

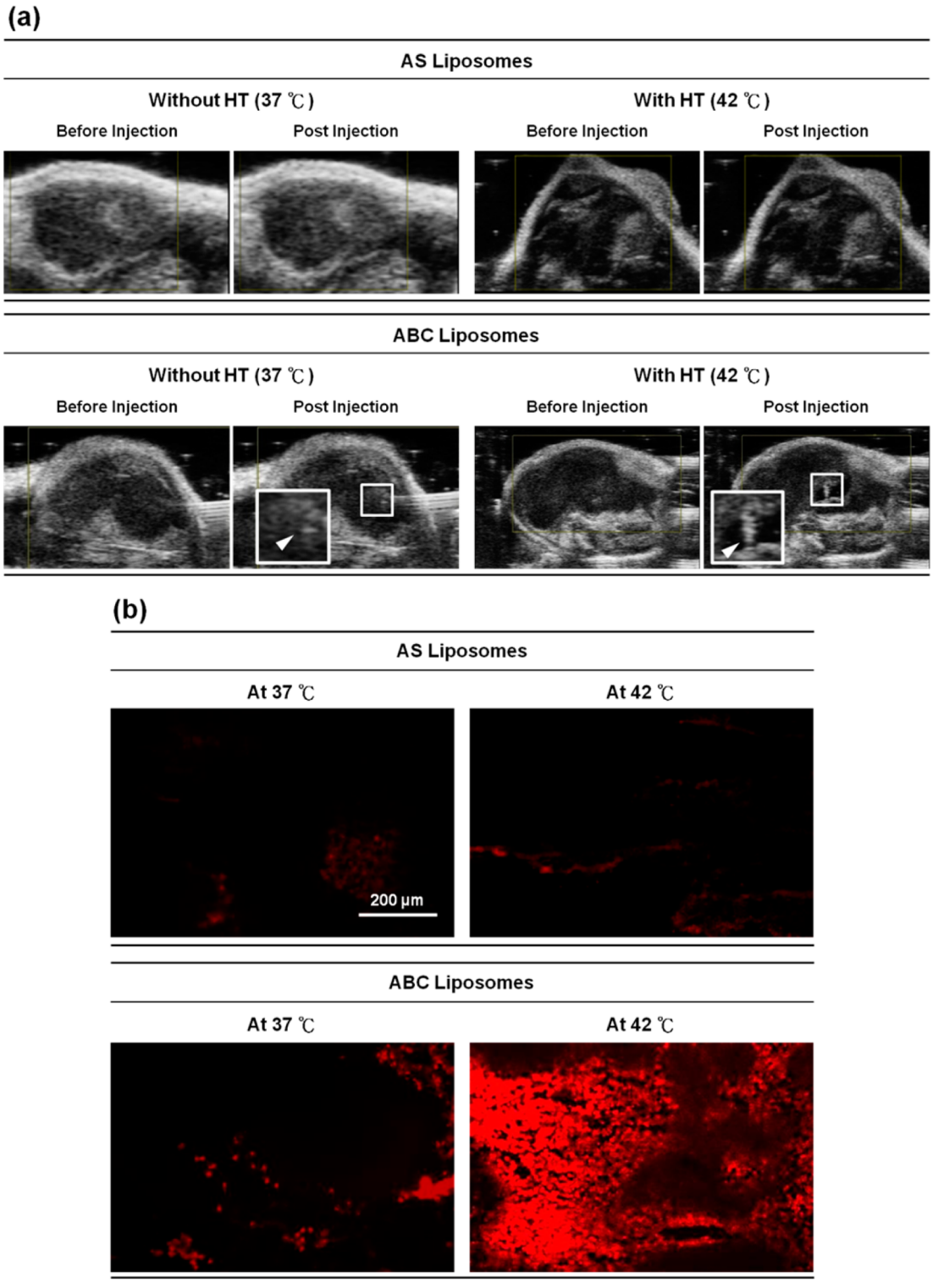

Figure 6. (a) Ultrasound images of the tumors treated with the AS or ABC liposomes at the body (37 °C) and hyperthermic temperatures (42 °C). Area denoted by a square appears at a higher magnification in the inset. HT: hyperthermia treatment. (b) Fluorescent images of DOX of the frozen tumor sections following intratumoral injection of the AS or ABC liposomes at the body (37 °C) and elevated temperatures (42 °C).

liver and kidney with (42 °C) or without (37 °C) hyperthermia treatment. No apparent DOX signal in the heart was detected for both test liposomes, suggesting that DOX-related cardiomyopathy can be reduced upon using liposomal formulations of the drug.[41] In mice receiving the AS liposomes, minimal DOX fluorescence signals appeared in tumors at both test temperatures, indicating that the release of their encapsulated DOX is limited and temperature-independent. Conversely, in the group receiving the ABC liposomes

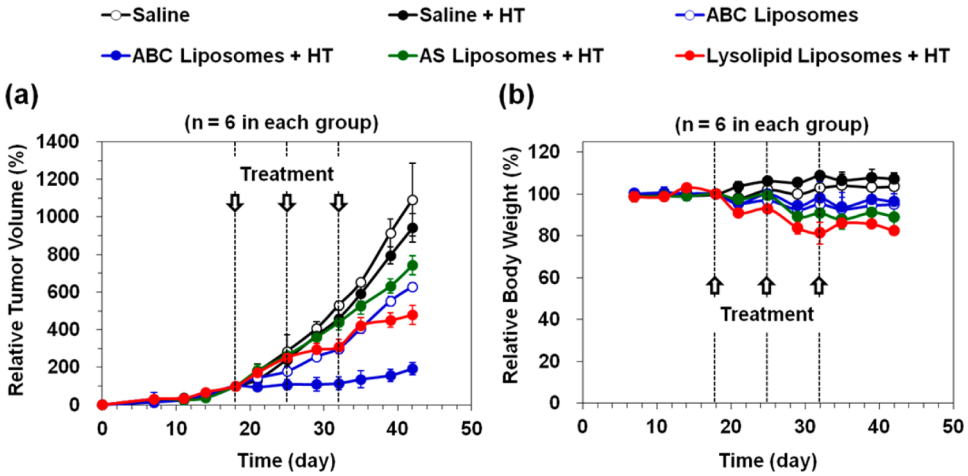

Figure 7. Changes in relative (a) tumor volume and (b) body weight of mice bearing tumors after the intravenous administration with different liposomal formulations under local hyperthermia treatment (HT).

without hyperthermia treatment, the strength of DOX fluorescence was relatively low. However, increasing the local temperature to 42 °C significantly enhanced the fluorescence signal ($P < 0.05$). Theoretically, when DOX is encapsulated at high concentrations in liposomes, its fluorescence signal is quenched, and release of the drug increases the fluorescence intensity.[42] These imaging findings demonstrate that DOX molecules are retained relatively tightly inside the ABC liposomes at body temperature. However, when mild heating was applied, decomposition of their encapsulated ABC facilitated immediate thermal activation of CO_2 bubble generation, leading to a marked release of DOX molecules.

Despite an investigation of the thermal activation of CO_2 bubble generation from the intratumoral ABC liposomes by an ultrasound machine, no apparent ultrasound signal was detected. This is likely because the amount of ABC liposomes accumulated in tumors was inadequate, explaining why the quantity of CO_2 bubbles generated was below the sensitivity of the ultrasound machine. As is well-known, the amount of intravenously administered nanocarriers delivered to tumor targets *via* the EPR effect is usually less than 5%.[43]

***In Vivo* Thermal Activation of CO_2 Bubble Generation and DOX Release.** An attempt was made to confirm the ability of the ABC liposomes to generate CO_2 bubbles at defined sites *in vivo* under mild hyperthermia. Test mice were intratumorally injected with an ABC liposomal suspension (5 mg liposomes/kg) after heating the tumor sites locally to 42 °C for 10 min. Their AS counterparts served as the control. No heat was applied during ultrasound examination.[44]

According to Figure 6a and Supporting Information video 1, no ultrasound contrast was apparent for the group receiving the AS liposomes at both body (37 °C) and hyperthermic temperatures (42 °C). Conversely, upon the intratumoral injection of the ABC liposome suspension, poor imaging signals were identified in the ultrasound scan (denoted by the white arrowhead) at 37 °C. Considerably stronger ultrasound signals (1.5-fold stronger in intensity, as analyzed by ImageJ) were observed when local temperature was heated to 42 °C (Supporting Information video 2). Above imaging results reveal that decomposition of the ABC encapsulated in liposomes facilitates immediate thermal activation of CO_2 bubble generation.

To investigate the intratumoral release of DOX from the test liposomes, tumor sections were examined histologically. In tumor sections receiving the AS liposomes, minimal fluorescence signals existed at both test temperatures, indicating that the release of their encapsulated DOX was limited and temperature-independent (Figure 6b). Conversely, in the group treated with the ABC liposomes, a few fluorescence spots were found at 37 °C; however, as local temperature was elevated to 42 °C, the strength and distribution of fluorescence signals increased. These imaging findings demonstrate that DOX molecules were retained relatively tightly inside the ABC liposomes at body temperature; however, when mild heating was applied, a marked release of DOX molecules occurred locally. That is, the combination of local heating and thermoresponsive ABC liposomes increased intratumoral free drug concentrations.

Antitumor Efficacy. Finally, the ability of different liposomal formulations to suppress tumor growth in mice was examined by using the same procedure in the study of *in vivo* DOX accumulation. In contrast to their counterparts without local heating, tumor growth in the saline-injected mice with local hyperthermia was slightly suppressed yet statistically insignificant ($P > 0.05$; Figure 7a), indicating that the effect of local heating was negligible. The effect of heat cytotoxicity can be isolated by examining the saline groups with or without local hyperthermia treatment.[44]

Combined with local heating, the thermoresponsive lysolipid liposomes had a better antitumor activity than the temperature-insensitive AS liposomal formulation ($P < 0.05$), indicating the importance of DOX release from the carriers. According to the *in vitro* drug-release study, the amount of DOX released from the lysolipid liposomes (70%) was significantly higher than that from AS liposomes (5%) under mild hyperthermia conditions (Figure 2).

In the case of the ABC liposomes combined with local heating, tumor growth was more significantly suppressed than that of the ABC liposomes without heat treatment ($P < 0.05$). This finding reveals that the pharmaceutical effect of the ABC liposomes at elevated temperature (42 °C) is more efficient than at body temperature since considerably more DOX molecules were released and accumulated in tumor cells (Figure 5a,b). Maximum therapeutic effects can only be achieved when tumor cells are subject to maximum drug exposure.[45] Notably, the antitumor efficacy of the thermoresposive ABC liposomes was superior to that of lysolipid liposomes ($P < 0.05$). This difference is because the extent of drug accumulation at the target tumor delivered by the ABC liposomes was higher than that *via* the lysolipid liposomes, as demonstrated in our biodistribution study (Figure 3a,b).

The body weight of test mice was also evaluated since it reflects the general toxicity of different delivery formulations.[46] The mice receiving the lysolipid liposomes had a significantly higher toxicity (or lost more original body weight) than those treated with the AS or ABC liposomes (Figure 7b). Analytical results demonstrate that the ABC liposomes, with their greater kinetic stability, delivered DOX to the tumor more effectively than the lysolipid formulation, thereby reducing the toxicity caused by the nonspecificity of DOX.

CONCLUSIONS

This study demonstrates the feasibility of using the proposed bubble-generating ABC liposomal system to release drugs locally under mild hyperthermia. The proposed system can also significantly improve DOX accumulation in tumor tissues. The highly thermoresponsive properties of the ABC liposomes contribute to efforts to establish effective tumor-selective chemotherapy.

EXPERIMENTAL SECTION

Materials. DPPC, MSPC, and PEG 2000-DSPE were purchased from Avanti Polar Lipids (Alabaster, AL, USA), while DOX was obtained from Fisher Scientific (Waltham, MA, USA). AS, ABC, and cholesterol were purchased from Sigma-Aldrich (St. Louis, MO, USA). All other chemicals and reagents used were of analytical grade.

Liposome Preparation. Test liposomes were prepared by using the thin-film hydration method, followed by membrane extrusion.[47,48] Briefly, lipids were dissolved in chloroform and placed under high vacuum pressure to remove the residual organic solvent. The lipid film was then hydrated (10 mg/mL) with an aqueous AS (350 mM) or ABC (2.7 M) solution *via* sonication at room temperature, followed by sequential extrusions through 800, 400, 200, and 100 nm polycarbonate filters (six times each) for size control at room temperature. The lipid recovery rate following multiple extrusions was approximately 90%, determined by a lipid phosphate assay.[49] The free AS or ABC was removed by dialyzing against 10 wt % sucrose solution with 5 mM NaCl. DOX was subsequently mixed with the liposome suspension at a drug/lipid ratio of 0.05 (w/w) and maintained at room temperature for 24 h. Finally, liposomes were passed through another G-50 column (GE Healthcare, Buckinghamshire, UK) to remove the unencapsulated DOX.

Characterization of Test Liposomes. The particle size, polydispersity index, and zeta-potential of the test liposomes were determined by dynamic light scattering (Zetasizer 3000HS; Malvern Instruments, Worcestershire, UK). The encapsulated DOX concentration in each liposomal formulation was measured using fluorescence measurements (Spex FluoroMax-3; Horiba Jobin Yvon, Edison, NJ, USA) after destroying the liposomes with Triton X-100. Finally, T_m of the lipid membranes was evaluated with a DSC (Q2000 DSC; TA Instruments, USA) during heating at 1 °C/min from 20 to 70 °C.[50]

***In Vitro* Release of DOX from Test Liposomes.** DOX release profiles were obtained by immersing the test liposomes (10 mg/mL, 50 μL) in quartz cells containing 1 mL of PBS. The amount of DOX released from the test liposomes at 37 or 42 °C was determined by measuring its fluorescence intensity at 485 nm using a fluorescence spectrometer at various time intervals. Upon completion of each measurement, 5 μL of a 10% v/v solution of Triton X-100 was added to a 1 mL solution in order to disrupt the test liposomes. The percentage of DOX released was calculated as $(I_t - I_0)/(I_{100} - I_0) \times 100\%$, in which I_t denotes fluorescence intensity at a specific time (t); I_0 represents fluorescence intensity at $t = 0$; and I_{100} refers to fluorescence intensity after adding Triton X-100.[50]

Animals and Tumor Cells. Nude mice (BALB/cAnN.Cg-Foxn1nu/CrlNarl, 6–8 weeks old) were purchased from the National Laboratory Animal Center, Taiwan. Use and care of experimental animals were in compliance with the "Guide for the Care and Use of Laboratory Animals" prepared by the Institute of Laboratory Animal Resources, National Research Council and published by the National Academy Press in 1996, and approved by the Institutional Animal Care and Use Committee of National Tsing Hua University (Protocol No. 10177). The human lung cancer cell line H460 was obtained from the Bioresource Collection and Research Center, Food Industry Research and Development Institute, Hsinchu, Taiwan. The H460 cells were maintained in RPMI 1640 medium supplemented with 10% fetal bovine serum, pH 7.4 at 37 °C in a humidified incubation chamber with 5% CO_2. Finally, the H460 cells were implanted subcutaneously (5×10^6 cells in 50 mL of PBS) in the right flank region of athymic nude mice and grown for approximately 18 days to an average volume of 200 mm^3.[51]

SPECT/CT Imaging. Details of the methods to prepare the ^{99m}Tc-liposomes can be found elsewhere.[32] SPECT/CT imaging was performed on a NanoSPECT/CT small-animal scanner equipped with four 1.5 mm multipinhole collimators (Bioscan, Washington, DC. USA). Test tumor-bearing mice were injected intravenously with ^{99m}Tc-lysolipid liposomes, ^{99m}Tc-AS liposomes, or ^{99m}Tc-ABC liposomes ($n = 3$ in each group, 300 μCi/100 μL, 100 μL); the SPECT/CT images were then taken at the desired time points. Finally, the strengths of radioactivity accumulated in internal organs were examined by using an image analysis software (PMOD Technologies, Zurich, Switzerland) and expressed as percentage of injected dose per milliliter (% ID/mL).

Plasma Stability Assay. Following incubation of the DOX-loaded liposomes with rat whole blood (Sprague–Dawley, 6–8 weeks old) at various time intervals at 37 °C, blood cells

were first separated from plasma by centrifugation. The plasma samples were then passed through G-50 columns to separate free DOX released from liposomes. To disrupt the test liposomes and evaluate the DOX plasma level, 10 μL plasma was diluted with 990 μL acidified isopropyl alcohol, and the mixture was incubated overnight at 4 °C in darkness. The samples were then centrifuged for 10 min at 12 000*g*. Finally, fluorescence intensity of the solution was monitored with a fluorescence spectrometer, which was expressed as a percentage of DOX retained in test liposomes.[14]

***In Vivo* DOX Accumulation.** Test AS and ABC liposomes were individually injected intravenously *via* the tail vein in mice bearing H460 tumors. At 4 h after treatments, mice were sacrificed, and their organs and tumors were harvested and visualized by an IVIS imaging system (Xenogen, Alameda, CA, USA). An aqueous solution (10 mL) containing deionized water and ethanol (50/50 by v/v) was subsequently added to each test tissue. The mixture was then homogenized and centrifuged at 14 000 rpm for 30 min; the supernatant was lyophilized and resuspended in 1 mL of deionized water. Finally, the fluorescence intensity of the solution was determined using a spectrofluorometer (F-2500, Hitachi, Tokyo, Japan).

Ultrasound/Fluorescence Imaging of Tumor Tissues. Tumor-bearing mice were anesthetized using pentobarbital and placed on a warm mat with 42 °C circulating water for 10 min prior to the experiment.[52] The nude mice were then intratumorally injected with a 10 μL ABC liposome suspension (10 mg/mL) before ultrasound examination; the AS liposomes were a control (n = 3 in each group). Ultrasound imaging was performed with a dedicated small-animal high spatial resolution imaging system (Vevo 2100; VisualSonics, Toronto, Canada). An 18 MHz linear transducer (gain = 25 dB; frame rate = 25 Hz; dynamic range = 25 dB) was attached on a rail system. Real-time imaging was obtained at a frame rate of 10 Hz.[53] After treatment, mice were sacrificed and their tumors were harvested and frozen at −80 °C until further sectioning. Accumulation of DOX in tumors was visualized by fluorescence microscopy (Axio Observer; Carl Zeiss, Jena, Germany) of frozen tissues cryo-sectioned at 5−7 μm thicknesses.

Antitumor Efficacy Study. Test liposomes encapsulating DOX were injected intravenously *via* the tail vein (5 mg/kg/week) for 3 weeks (n = 6 in each group) in mice bearing tumors. Tumor volume and body weight were measured at regular intervals. Tumor size was identified with a caliper. Tumor volume was calculated using the following equation: $V = (\pi/6) \times LW^2$, where L denotes long diameter and W represents short diameter.[54]

Statistical Analysis. All results are presented as mean ± SD. Student t test was performed to compare the mean of two groups. A comparison of more than two groups was analyzed by one-way ANOVA followed by Bonferroni post hoc test. Differences were considered statistically significant when $P < 0.05$.

Conflict of Interest: The authors declare no competing financial interest.

Acknowledgment. The authors would like to thank the National Science Council of the Republic of China, Taiwan, for financially supporting this research under Contract Nos. NSC 101-2120-M-007-015-CC1 and NSC 101-2221-E-182-002-MY3. Chang Gung Memorial Hospital (Linkou, Taiwan) is also commended for partially supporting the molecular-imaging study under Contract Nos. CMRP391513 and CMRPG3A0512.

Supporting Information Available: Supplementary video 1: ultrasound images of the tumor after treated with the AS liposomes at an elevated temperature of 42 °C. Supplementary video 2: ultrasound images of the tumor after treated with the ABC liposomes at an elevated temperature of 42 °C. This material is available free of charge *via* the Internet at http://pubs.acs.org.

REFERENCES AND NOTES

1. Barenholz, Y. Doxil—The First FDA-Approved Nano-Drug: Lessons Learned. *J. Controlled Release* **2012**, *160*, 117–134.
2. Yang, F.; Jin, C.; Jiang, Y.; Li, J.; Di, Y.; Ni, Q.; Fu, D. Liposome Based Delivery Systems in Pancreatic Cancer Treatment: From Bench to Bedside. *Cancer Treat. Rev.* **2011**, *37*, 633–642.
3. Elbayoumi, T. A.; Torchilin, V. P. Tumor-Targeted Nanomedicines: Enhanced Antitumor Efficacy *in Vivo* of Doxorubicin-Loaded, Long-Circulating Liposomes Modified with Cancer-Specific Monoclonal Antibody. *Clin. Cancer Res.* **2009**, *15*, 1973–1980.
4. Pornpattananangkul, D.; Olson, S.; Aryal, S.; Sartor, M.; Huang, C. M.; Vecchio, K.; Zhang, L. Stimuli-Responsive Liposome Fusion Mediated by Gold Nanoparticles. *ACS Nano* **2010**, *4*, 1935–1942.
5. Allen, T. M.; Cullis, P. R. Drug Delivery Systems: Entering the Mainstream. *Science* **2004**, *303*, 1818–1822.
6. Kong, G.; Anyarambhatla, G.; Petros, W. P.; Braun, R. D.; Colvin, O. M.; Needham, D.; Dewhirst, M. W. Efficacy of Liposomes and Hyperthermia in a Human Tumor Xenograft Model: Importance of Triggered Drug Release. *Cancer Res.* **2000**, *15*, 6950–6957.
7. Chang, H. I.; Yeh, M. K. Clinical Development of Liposome-Based Drugs: Formulation, Characterization, and Therapeutic Efficacy. *Int. J. Nanomed.* **2012**, *7*, 49–60.
8. Dromi, S.; Frenkel, V.; Luk, A.; Traughber, B.; Angstadt, M.; Bur, M.; Poff, J.; Xie, J.; Libutti, S. K.; Li, K. C.; *et al.* Pulsed-High Intensity Focused Ultrasound and Low Temperature-Sensitive Liposomes for Enhanced Targeted Drug Delivery and Antitumor Effect. *Clin. Cancer Res.* **2007**, *13*, 2722–2727.
9. Shenoi, M. M.; Shah, N. B.; Griffin, R. J.; Vercellotti, G. M.; Bischof, J. C. Nanoparticle Pre-conditioning for Enhanced Thermal Therapies in Cancer. *Nanomedicine* **2011**, *6*, 545–563.
10. Yarmolenko, P. S.; Zhao, Y.; Landon, C.; Spasojevic, I.; Yuan, F.; Needham, D.; Viglianti, B. L.; Dewhirst, M. W. Comparative Effects of Thermosensitive Doxorubicin-Containing Liposomes and Hyperthermia in Human and Murine Tumours. *Int. J. Hyperthermia* **2010**, *26*, 485–498.
11. Tagami, T.; Foltz, W. D.; Ernsting, M. J.; Lee, C. M.; Tannock, I. F.; May, J. P.; Li, S. D. MRI Monitoring of Intratumoral Drug Delivery and Prediction of the Therapeutic Effect with a Multifunctional Thermosensitive Liposome. *Biomaterials* **2011**, *32*, 6570–6578.
12. Tagami, T.; Ernsting, M. J.; Li, S. D. Optimization of a Novel and Improved Thermosensitive Liposome Formulated with DPPC and a Brij Surfactant Using a Robust *In Vitro* System. *J. Controlled Release* **2011**, *154*, 290–297.
13. Chiu, G. N.; Abraham, S. A.; Ickenstein, L. M.; Ng, R.; Karlsson, G.; Edwards, K.; Wasan, E. K.; Bally, M. B. Encapsulation of Doxorubicin into Thermosensitive Liposomes *via* Complexation with the Transition Metal Manganese. *J. Controlled Release* **2005**, *104*, 271–288.
14. Banno, B.; Ickenstein, L. M.; Chiu, G. N.; Bally, M. B.; Thewalt, J.; Brief, E.; Wasan, E. K. The Functional Roles of Poly(ethylene glycol)−Lipid and Lysolipid in the Drug Retention and Release from Lysolipid-Containing Thermosensitive Liposomes *in Vitro* and *in Vivo*. *J. Pharm. Sci.* **2010**, *99*, 2295–2308.
15. Chen, K. J.; Liang, H. F.; Chen, H. L.; Wang, Y.; Cheng, P. Y.; Liu, H. L.; Xia, Y.; Sung, H. W. A Thermoresponsive Bubble-Generating Liposomal System for Triggering Localized Extracellular Drug Delivery. *ACS Nano* **2013**, *7*, 438–446.
16. Chung, M. F.; Chen, K. J.; Liang, H. F.; Liao, Z. X.; Chia, W. T.; Xia, Y.; Sung, H. W. A New Liposomal System Capable of Generating CO_2 Bubbles To Induce Transient Cavitation, Lysosomal Rupturing, and Cell Necrosis. *Angew. Chem., Int. Ed.* **2012**, *51*, 10089–10093.
17. Boddien, A.; Gärtner, F.; Federsel, C.; Sponholz, P.; Mellmann, D.; Jackstell, R.; Junge, H.; Beller, M. CO_2-"Neutral" Hydrogen Storage Based on Bicarbonates and Formates. *Angew. Chem., Int. Ed.* **2011**, *50*, 6411–6414.
18. Yang, Y.; Bajaj, N.; Xu, P.; Ohn, K.; Tsifansky, M. D.; Yeo, Y. Development of Highly Porous Large PLGA Microparticles for Pulmonary Drug Delivery. *Biomaterials* **2009**, *30*, 1947–1953.
19. Min, B.; Bae, I. Y.; Lee, H. G.; Yoo, S. H.; Lee, S. Utilization of Pectin-Enriched Materials from Apple Pomace as a Fat Replacer in a Model Food System. *Bioresour. Technol.* **2010**, *101*, 5414–5418.
20. Romero, M. F.; Chen, A. P.; Parker, M. D.; Boron, W. F. The SLC4 Family of Bicarbonate (HCO_3^-) Transporters. *Mol. Aspects Med.* **2013**, *34*, 159–182.

21. Martin, N. K.; Gaffney, E. A.; Gatenby, R. A.; Gillies, R. J.; Robey, I. F.; Maini, P. K. A Mathematical Model of Tumour and Blood pH Regulation: The HCO_3^-/CO_2 Buffering System. *Math. Biosci.* **2011**, *230*, 1–11.
22. Landon, C. D.; Park, J. Y.; Needham, D.; Dewhirst, M. W. Nanoscale Drug Delivery and Hyperthermia: The Materials Design and Preclinical and Clinical Testing of Low Temperature-Sensitive Liposomes Used in Combination with Mild Hyperthermia in the Treatment of Local Cancer. *Open Nanomed. J.* **2011**, *3*, 38–64.
23. Cern, A.; Golbraikh, A.; Sedykh, A.; Tropsha, A.; Barenholz, Y.; Goldblum, A. Quantitative Structure−Property Relationship Modeling of Remote Liposome Loading of Drugs. *J. Controlled Release* **2012**, *160*, 147–157.
24. Tagami, T.; May, J. P.; Ernsting, M. J.; Li, S. D. A Thermosensitive Liposome Prepared with a Cu^{2+} Gradient Demonstrates Improved Pharmacokinetics, Drug Delivery and Antitumor Efficacy. *J. Controlled Release* **2012**, *161*, 142–149.
25. Bolotin, E. M.; Cohen, R.; Bar, L.; Emanuel, N.; Ninio, S.; Barenholz, Y.; Lasic, D. D. Ammonium Sulfate Gradients for Efficient and Stable Remote Loading of Amphipathic Weak Bases into Liposomes and Ligandoliposomes. *J. Liposome Res.* **1994**, *4*, 455–479.
26. James, M. L.; Gambhir, S. S. A Molecular Imaging Primer: Modalities, Imaging Agents, and Applications. *Physiol. Rev.* **2012**, *2*, 897–965.
27. Gomes, C. M.; Abrunhosa, A. J.; Ramos, P.; Pauwels, E. K. Molecular Imaging with SPECT as a Tool for Drug Development. *Adv. Drug Delivery Rev.* **2011**, *63*, 547–554.
28. Bao, A.; Goins, B.; Klipper, R.; Negrete, G.; Phillips, W. T. Direct ^{99m}Tc Labeling of PEGylated Liposomal Doxorubicin (Doxil) for Pharmacokinetic and Non-invasive Imaging Studies. *J. Pharmacol. Exp. Ther.* **2004**, *308*, 419–425.
29. Goins, B.; Bao, A.; Phillips, W. T. Techniques for Loading Technetium-99m and Rhenium-186/188 Radionuclides into Pre-formed Liposomes for Diagnostic Imaging and Radionuclide Therapy. *Methods Mol. Biol.* **2010**, *606*, 469–491.
30. Li, S.; Goins, B.; Hrycushko, B. A.; Phillips, W. T.; Bao, A. Feasibility of Eradication of Breast Cancer Cells Remaining in Postlumpectomy Cavity and Draining Lymph Nodes Following Intracavitary Injection of Radioactive Immunoliposomes. *Mol. Pharmacol.* **2012**, *9*, 2513–2252.
31. Sonaje, K.; Lin, K. J.; Wey, S. P.; Lin, C. K.; Yeh, T. H.; Nguyen, H. N.; Hsu, C. W.; Yen, T. C.; Juang, J. H.; Sung, H. W. Biodistribution, Pharmacodynamics and Pharmacokinetics of Insulin Analogues in a Rat Model: Oral Delivery Using pH-Responsive Nanoparticles *vs.* Subcutaneous Injection. *Biomaterials* **2010**, *31*, 6849–6858.
32. Matsuzaki, T.; Takagi, A.; Furuta, T.; Ueno, S.; Kurita, A.; Nohara, G.; Kodaira, H.; Sawada, S.; Hashimoto, S. Antitumor Activity of IHL-305, a Novel PEGylated Liposome Containing Irinotecan, in Human Xenograft Models. *Oncol. Rep.* **2012**, *27*, 189–197.
33. Lowery, A.; Onishko, H.; Hallahan, D. E.; Han, Z. Tumor-Targeted Delivery of Liposome-Encapsulated Doxorubicin by Use of a Peptide that Selectively Binds to Irradiated Tumors. *J. Controlled Release* **2011**, *150*, 117–124.
34. Hiraoka, M.; Masunaga, S.; Nishimura, Y.; Nagata, Y.; Jo, S.; Akuta, K.; Li, Y. P.; Takahashi, M.; Abe, M. Regional Hyperthermia Combined with Radiotherapy in The Treatment of Lung Cancers. *Int. J. Radiat. Oncol., Biol., Phys.* **1992**, *22*, 1009–1014.
35. Karasawa, K.; Muta, N.; Nakagawa, K.; Hasezawa, K.; Terahara, A.; Onogi, Y.; Sakata, K.; Aoki, Y.; Sasaki, Y.; Akanuma, A. Thermoradiotherapy in the Treatment of Locally Advanced Nonsmall Cell Lung Cancer. *Int. J. Radiat. Oncol., Biol., Phys.* **1994**, *30*, 1171–1177.
36. Daemen, T.; Velinova, M.; Regts, J.; de Jager, M.; Kalicharan, R.; Donga, J.; van der Want, J. J.; Scherphof, G. L. Different Intrahepatic Distribution of Phosphatidylglycerol and Phosphatidylserine Liposomes in the Rat. *Hepatology* **1997**, *26*, 416–423.
37. Hilmer, S. N.; Cogger, V. C.; Muller, M.; Le Couteur, D. G. The Hepatic Pharmacokinetics of Doxorubicin and Liposomal Doxorubicin. *Drug Metab. Dispos.* **2004**, *32*, 794–799.
38. Maruyama, K. Intracellular Targeting Delivery of Liposomal Drugs to Solid Tumors Based on EPR Effects. *Adv. Drug Delivery Rev.* **2011**, *63*, 161–169.
39. Kono, K.; Ozawa, T.; Yoshida, T.; Ozaki, F.; Ishizaka, Y.; Maruyama, K.; Kojima, C.; Harada, A.; Aoshima, S. Highly Temperature-Sensitive Liposomes Based on a Thermosensitive Block Copolymer for Tumor-Specific Chemotherapy. *Biomaterials* **2010**, *27*, 7096–7105.
40. Greco, A.; Di Benedetto, A.; Howard, C. M.; Kelly, S.; Nande, R.; Dementieva, Y.; Miranda, M.; Brunetti, A.; Salvatore, M.; Claudio, L.; *et al.* Eradication of Therapy-Resistant Human Prostate Tumors Using an Ultrasound-Guided Site-Specific Cancer Terminator Virus Delivery Approach. *Mol. Ther.* **2010**, *2*, 295–306.
41. Waterhouse, D. N.; Tardi, P. G.; Mayer, L. D.; Bally, M. B. A Comparison of Liposomal Formulations of Doxorubicin with Drug Administered in Free Form: Changing Toxicity Profiles. *Drug Saf.* **2001**, *24*, 903–920.
42. Laginha, K. M.; Verwoert, S.; Charrois, G. J.; Allen, T. M. Determination of Doxorubicin Levels in Whole Tumor and Tumor Nuclei in Murine Breast Cancer Tumors. *Clin. Cancer Res.* **2005**, *11*, 6944–6949.
43. Bae, Y. H.; Park, K. Targeted Drug Delivery to Tumors: Myths, Reality and Possibility. *J. Controlled Release* **2011**, *10*, 198–205.
44. Ke, C. J.; Su, T. Y.; Chen, H. L.; Liu, H. L.; Chiang, W. L.; Chu, P. C.; Xia, Y.; Sung, H. W. Smart Multifunctional Hollow Microspheres for the Quick Release of Drugs in Intracellular Lysosomal Compartments. *Angew. Chem., Int. Ed.* **2011**, *50*, 8086–8089.
45. Allen, T. M. Ligand-Targeted Therapeutics in Anticancer Therapy. *Nat. Rev. Cancer* **2002**, *2*, 750–763.
46. Klimtová, I.; Simunek, T.; Mazurová, Y.; Hrdina, R.; Gersl, V.; Adamcová, M. Comparative Study of Chronic Toxic Effects of Daunorubicin and Doxorubicin in Rabbits. *Hum. Exp. Toxicol.* **2002**, *12*, 649–657.
47. Soussan, E.; Cassel, S.; Blanzat, M.; Rico-Lattes, I. Drug Delivery by Soft Matter: Matrix and Vesicular Carriers. *Angew. Chem., Int. Ed.* **2009**, *48*, 274–288.
48. Boyer, C.; Zasadzinski, J. A. Multiple Lipid Compartments Slow Vesicle Contents Release in Lipases and Serum. *ACS Nano* **2007**, *1*, 176–182.
49. Bartlett, G. R. Phosphorus Assay in Column Chromatography. *J. Biol. Chem.* **1959**, *234*, 466–468.
50. de Smet, M.; Langereis, S.; van den Bosch, S.; Grüll, H. Temperature-Sensitive Liposomes for Doxorubicin Delivery under MRI Guidance. *J. Controlled Release* **2010**, *143*, 120–127.
51. Teicher, B. A.; Chen, V.; Shih, C.; Menon, K.; Forler, P. A.; Phares, V. G.; Amsrud, T. Treatment Regimens Including the Multitargeted Antifolate LY231514 in Human Tumor Xenografts. *Clin. Cancer Res.* **2000**, *3*, 1016–1023.
52. Ranjan, A.; Jacobs, G. C.; Woods, D. L.; Negussie, A. H.; Partanen, A.; Yarmolenko, P. S.; Gacchina, C. E.; Sharma, K. V.; Frenkel, V.; Wood, B. J.; *et al.* Image-Guided Drug Delivery with Magnetic Resonance Guided High Intensity Focused Ultrasound and Temperature Sensitive Liposomes in a Rabbit Vx2 Tumor Model. *J. Controlled Release* **2012**, *158*, 487–494.
53. Negishi, Y.; Hamano, N.; Tsunoda, Y.; Oda, Y.; Choijamts, B.; Endo-Takahashi, Y.; Omata, D.; Suzuki, R.; Maruyama, K.; Nomizu, M.; *et al.* AG73-Modified Bubble Liposomes for Targeted Ultrasound Imaging of Tumor Neovasculature. *Biomaterials* **2013**, *2*, 501–507.
54. Ahn, R. W.; Chen, F.; Chen, H.; Stern, S. T.; Clogston, J. D.; Patri, A. K.; Raja, M. R.; Swindell, E. P.; Parimi, V.; Cryns, V. L.; *et al.* A Novel Nanoparticulate Formulation of Arsenic Trioxide with Enhanced Therapeutic Efficacy in a Murine Model of Breast Cancer. *Clin. Cancer Res.* **2010**, *16*, 3607–3617.